View metadata, citation and similar papers at core.ac.uk

brought to you by CORE

provided by Elsevier - Publisher Connector

Sensing and Bio-Sensing Research 4 (2015) 61–69

Contents lists available at ScienceDirect

Sensing and Bio-Sensing Research

journal homepage: www.elsevier.com/locate/sbsr

Increasing performance and stability of mass-manufacturable biobatteries by ink modification

Saara Tuurala [a,*], Tanja Kallio [b], Maria Smolander [a], Mikael Bergelin [c]

[a] VTT Technical Research Centre of Finland, Tietotie 3, Espoo, FI-02044 VTT, Finland
[b] Department of Chemistry, Aalto University, P.O. Box 16100, FI-00076 AALTO, Finland
[c] Åbo Akademi, Process Chemistry Centre, Biskopsgatan 8, FI-20500 Åbo, Finland

ARTICLE INFO

Keywords:
Enzymatic electrode
Self-powered biosensor
Biobattery
Stability
Mass-manufacturing
Printing

ABSTRACT

In this work, biobatteries assembled using roll-to-roll screen printed enzymatic electrodes were characterised in terms of their electrical performance and storage stability. The enzymes and mediators used on the anode and cathode were glucose oxidase with ferrocenemethanol and laccase with ABTS, respectively. This study shows that besides rheological properties of enzyme inks used for the printing of the biobattery electrodes also adhesion of these electrodes to the printing substrate can be adjusted by varying the amount and composition of the binder in the ink. Another important observation is that the mediator has a strong impact on both the performance and the stability of the anode electrode. Consequently, electrochemical performance of biobatteries can be enhanced by adding fresh mediator into the battery during activation or by some other method preserving the activity of the mediator. Hence, this study discusses and sheds light on important practical aspects for up-scaling production process of biobatteries and also other printed bioelectronics.

© 2015 The Authors. Published by Elsevier B.V. This is an open access article under the CC BY-NC-ND license (http://creativecommons.org/licenses/by-nc-nd/4.0/).

1. Introduction

Printing of enzymes on paper or cardboard can add valuable functionalities to the substrate. These functionalized paper-based products could be used in low-cost diagnostics [24,53], indicators [7,9,41] or bioelectronics. In bioelectronics the functionality of the device is typically based on catalytic reactions of enzymes or affinity sensing due to formation of specific antigen–antibody complexes [48]. Typical examples of bioelectronic devices are potentiometric and amperometric biosensors [6,10,21], and enzymatic power sources [5].

Traditional amperometric biosensors require an external power supply for the signal-reading because the current generated in the detection reaction of the sensor is measured at controlled potential versus reference electrode. However, power supplies (e.g. batteries) are difficult to miniaturise. In addition, sensor designs allowing easy replacement or recharging of the battery are bulky. Another challenge in designing amperometric biosensors is interference current resulting from nonspecific redox reactions of other redox-active species upon application of potential on the working electrode.

In order to solve the challenges described above, biobattery configuration consisting of two electrodes has been introduced as a self-powered biosensor (SPB) device [1,18,57]. The operational principle of SPB is very simple; there is no voltage or current in the absence of the fuel, but the presence of the fuel in the anode induces voltage and current, and thus generates power. The induced current density and thus the power density are functions of the concentration of the fuel. Hence, the sensor itself provides the power for the sensing device when achieving the analytical signal. Still, in order to make SPBs as commercial products their electrical performance and stability need to be ensured. In addition, their mass-manufacturability has to be tested, and especially paper-based biosensors have drawn attention due to their inexpensive and renewable substrate material and disposability.

Although biocatalysts have been successfully applied on paper-based substrates possessing many desirable characteristics (including selectivity, non-toxicity, reproducibility and low-cost), their marginal stability has prevented or delayed their implementation for mass-manufacturing. As enzymes are removed from their natural environment and applied onto a paper-based surface, their hydration-level, pH and temperature are typically not optimal. For this reason their stability is poor. For an example, Khan et al. [20] reported half-lives of alkaline phosphatase (ALP) and horseradish peroxidase (HRP) adsorbed on paper of 22 days and 10 days at 23 °C, respectively, whereas ALP incubated at 37 °C in 50% glycerol solution is stable at least for 4 weeks and lyophilized HRP is stable at room temperature for 3 weeks (stability values are given by the enzyme manufacturers).

* Corresponding author. Tel.: +358 401843818.
E-mail address: saara.tuurala@vtt.fi (S. Tuurala).

http://dx.doi.org/10.1016/j.sbsr.2015.03.003
2214-1804/© 2015 The Authors. Published by Elsevier B.V.
This is an open access article under the CC BY-NC-ND license (http://creativecommons.org/licenses/by-nc-nd/4.0/).

The enzyme immobilization procedure is critical for the fabrication of enzymatic bioelectronics. The enzyme activity should be retained while favouring its electrical connection with the underlying conductive electrode material, directly or via a redox mediator. It has been seen that the bioelectrochemical interface in bioelectronic devices plays an important role in the performance of the device [56]. Immobilisation of enzymes into solid structures is one of the most used methods for stabilising enzymes [13,29]. This can be done by incorporating enzymes into printable inks and it is considered as one of the promising approaches for large-scale manufacturing processes for enzyme-containing electrodes. Hence, modification of the enzyme-containing inks in order to increase the enzymatic stability of the printed layers is an important challenge. One natural approach is to carefully select the solvents (usually water) and binders according to the enzymes used. For an example, Khan et al. [19] reported that water soluble polymers increased the adsorption of ALP on paper by around 50% and prevented enzyme desorption/leaching upon rewetting of the paper compared to non-treated paper. However, they also found out that the type of polymers affects the thermal stability and the ageing of ALP on paper, and in their case the thermal stability of ALP on paper decreased when polymers were used. For this reason, components of enzymatic inks must be chosen carefully.

We have previously demonstrated that biocatalyst-based electrodes can be produced on paper-based substrates by printing and in large scale [16,17,39,42,44]. In this work, biobattery assemblies using roll-to-roll (R2R) printed enzymatic electrodes were characterised by electrochemical methods. Storage stability was studied over one month period and optimisation of the printed anode was done by improving ink formulation. Rheological properties of enzyme containing inks and adhesion of these electrodes to the current collector can be adjusted by varying the amount and composition of the binder in the ink. Moreover, the mediator has a strong impact on both the performance and the stability of the anode electrode. Hence, this study reveals important practical aspects for up-scaling the printing production process of bioelectronics.

2. Material and methods

2.1. Materials

Materials for base inks were graphite powder (<20 μm, Aldrich 282863), polyethylene oxide (PEO, Aldrich 189456), and chitosan (Sigma 448877). The mediators and enzymes used in the inks were ferrocenemethanol (FeMeOH, Aldrich 335061), 2,2′-Azino-bis(3-ethylbenzothiazoline-6-sulfonic acid) diammonium salt (ABTS, Sigma A1888), glucose oxidase from *Aspergillus niger* (GOx, Sigma G7141) and laccase (EcoL, AB Enzymes Ecostone LCL 45, EC 1.10.3.2), respectively.

Materials for printing process and assembling the cells were polyethylene (PE) coated cardboard (Stora Enso Classic Bar PE 175 + 15 g/m^2), insulator paper (Delfortgroup, Terkab Ilam), current collector ink (Peters HAL SD-2843), dialysis membrane (Medicell International Ltd, visking code DTV12000.11.000), D-glucose (VWR 101176K) and succinic acid (Sigma–Aldrich 398055). The chemicals were used as received without further purification and distilled water was used in all the experiments.

2.2. Electrode preparation

2.2.1. Inks

A base ink was prepared by mixing graphite and binders (PEO and chitosan) together in different ratios as described in Table 1. The enzyme containing inks were prepared by mixing enzyme and mediator into the base ink. GOx and FeMeOH (dissolved in ethanol) were used for anode inks and EcoL and ABTS for the cathode inks. 50 mM Na-succinate buffer (pH 4.5) was used to adjust the viscosity of the ink (Table 1).

2.2.2. Printing and curing

Pilot printing trials were carried out using VTT's modular ROKO R2R pilot line (Fig. 1). The printing speed was 2 m min^{-1} and Gallus BY/RS Mesh 64 (thickness 200 μm) printing screens were used with all inks. PE-coated cardboard was used as the printing substrate and the ink was deposited on the PE-coated side. First, current collectors were printed using commercial carbon-based ink and cured on the printing line at 145 °C. The enzyme containing inks were printed as a separate layer (the geometrical electrode area was 9 cm^2) on top of the current collector layers and cured on the printing line at approximately 70 °C. The layers were cured using three 0.9 m long box ovens; hence the accumulative curing time was 81 s. The printed cardboard rolls (Fig. 2) were stored at room temperature. The first electrochemical measurements were performed after 1 week of manufacturing due to transportation from the pilot printing line to laboratory.

Experimental laboratory printing trials were carried out using a semi-automatic Kent SP-400 screen printer. The printing substrate was insulator paper (A4-size) and the screen mesh was NMC EX 31-100. The printed electrodes (the geometrical electrode area was 12.25 cm^2) were dried and stored at room temperature and characterised on the next day after manufacturing.

2.3. Cell assembly

Printed electrodes were stored at room temperature and cut from the printing substrate for assembly. As pilot-printed

Table 1
Compositions of enzymatic inks tested. The pilot anode ink 1 and cathode ink were prepared as previously published by Tuurala et al. [42] and the compositions are reprinted here with permission.

Component	Anode ink 1 for the 1st pilot run	Cathode ink for the pilot run	Experimental anode ink 1	Experimental anode ink 2	Experimental anode ink 3	Anode ink 2 for the 2nd pilot run
Graphite (g)	25	25	25	23	25	25
PEO (g) (5 wt% in H_2O)	18	18	18	16	35	35
Chitosan solution (g) (in 1% acetic acid)	–	–	4.3 different concentrations*	4 (1.5 wt%)	6.7 different concentrations*	7 (0.5 wt%)
Enzyme (nkat)	40,500	36,700	36,400	52,550	25,000	40,550
Mediator (mg) [μmol nkat^{-1}]	86 [0.01]	217 [0.01]	86 [0.01]	Different concentrations**	54 [0.01]	188 [0.02]
Solvent (ml) (ethanol)	0.4	0	0.4	0.4	0.4	0.6
Buffer (ml)	10–12	10–12	–	–	–	–

* Four different chitosan solutions were prepared: 0.5, 1.0, 1.5 and 2 wt% in 1% acetic acid and added into the experimental inks 1 and 3.
** Four different FeMeOH amounts were tested: 0.01, 0.03, 0.05 and 0.08 μmol nkat^{-1} (of GOx enzyme).

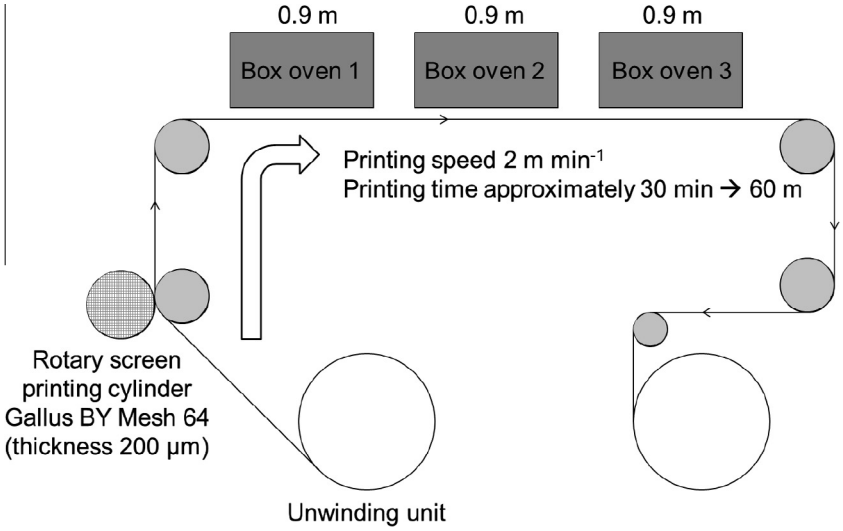

Fig. 1. Schematic of VTT's ROKO R2R pilot line. Printing of biobatteries can be seen in a YouTube video clip (https://www.youtube.com/watch?v=DS44BpavARk).

electrodes were characterised, anode (9 cm^2) was moisturised with 200 µl of 50 mM Na-succinate buffer (pH 4.5) and 50 mg of glucose. A piece of a dialysis membrane separator (16 cm^2) was set on top of the anode. Cathode (9 cm^2) was moisturised with 100 µl of buffer and assembled on top of the anode-separator layer so that the printed sides of the electrodes were facing each other. The cell assembly was fixed between planar graphite plates and the cell was connected to a potentiostat with alligator clips from the printed current collectors.

As the laboratory manufactured electrodes were assembled, anode (12.25 cm^2) and cathode (12.25 cm^2) were sandwiched between graphite current collector plates so that the printed sides of the electrodes were facing the graphite. Hence no additional separator was needed. There was a gasket (thickness 250 µm) between the anode and the cathode. The graphite plate on the cathode side had holes, and the cell was activated via the holes with 50 mg of glucose in 400 µl of buffer. The cell was connected to a potentiostat with alligator clips from the graphite current collectors.

2.4. Electrochemical measurements and data analysis

The electrochemical performance of the cells was measured using multichannel potentiostat (BioLogic VMP) in two electrode connection. At least three individual repetitions were measured and the error bars were calculated as standard error of the mean (SM). Student's *t*-test was used to evaluate the statistical significance between measurement sets. All the measurements are listed in Table 2.

In chronopotentiometry (CP) cells were measured at open circuit potential (OCP) for 1.5 h after which a constant current was drawn from the cells until the cell potential decreased to 0 V. The cell potential was recorded in 60 s intervals. The energy output of the cells was calculated by integrating the area until the cell potential decreased to (a) 200 mV and (b) 150 mV. In chronoamperometry (CA) cells were measured at OCP for 1.5 h after which the cell potential was decreased from 300 mV to 0 mV in 25 mV steps every 10 min. The steady state current was measured.

2.5. Characterisation of the morphology of the electrode

Thickness of the pilot printed electrodes was determined using a Dektak stylus profilometer. Roughness was measured using a Wyko white light interferometer and the area measured was 0.91 mm × 1.20 mm. Three Au layers were sputtered on top of the samples prior to measurement. The number of samples was at least three and three measurement points were analysed from each sample.

3. Results and discussion

3.1. Performance of the pilot anode ink 1

In our previous work we optimised the composition of the pilot inks in the perspective of the drying process on the ROKO R2R printing line [42]. However, the pilot anode ink 1 has a poor mechanical stability rendering assembling of the cells difficult. The ink has also high water-solubility which reduces the functionality and operational lifetime of the cell because the enzyme is not immobilized into the ink and the electrical conductivity is lost as the electrode wets. For this reason, the amount of binder was increased in the laboratory experimental inks (see Section 3.2).

As stability is one of the major issues in biobatteries, performance of the pilot cells was investigated. The OCP and the maximum power density of 1 week old pilot cells is (343 ± 4) mV and (0.40 ± 0.03) µW cm^{-2} (at 225 mV), respectively. The energy outputs of the 1 week old pilot cells are (0.59 ± 0.09) µW h cm^{-2} ($E_{cut\text{-}off}$ = 200 mV) and (0.67 ± 0.09) µW h cm^{-2} ($E_{cut\text{-}off}$ = 150 mV). Our fresh laboratory manufactured cells have an OCP of (380 ± 8) mV [42]. This data suggests that already 1 week of storing decreases the OCP and hence the power and energy outputs. After 10 weeks the performance of the cells has decreased close to zero, which can be seen in Fig. 3. The inset of Fig. 3 shows that in 10 weeks the OCP has decreased to 200 mV indicating that either the anodic and/or cathodic mediator is degrading.

In order to find out whether it is the anode or the cathode side of the cell that had degraded, 13 weeks old electrodes were tested against newly manufactured electrodes. The fresh electrodes were printed in laboratory on insulator paper using a semi-automatic screen printer. The results of the CP measurements are seen in Fig. 4a.

It can be seen that the cell performance is poor as both the anode and cathode are stored for 13 weeks. The same is observed with an aged anode and fresh cathode. In contrast, when a fresh anode was tested with an aged cathode the performance of the

Fig. 2. A roll of printed bioelectrodes on cardboard.

cells was significantly better. This indicates that the anode ageing is limiting the performance of the cells. This interpretation agrees with the results by Smolander et al. [39] and [50,51] where the enzymatic stability of printed laccase on a paper substrate is several months.

The next step was to investigate the degradation of the anode mediator. This was done by adding small amount of the fresh FeMeOH mediator into the activation electrolyte which was injected into the aged anodes. Addition of aged FeMeOH was also tested with electrolyte solutions prepared 1 and 2 weeks (stored at 4 °C) before the injection and measurement. Results of CP measurements with addition of fresh and aged FeMeOH via the activation electrolyte can be seen in Fig. 4b.

These measurements showed that by adding the fresh mediator solution on the anode side both OCP and energy output of the aged cells increases. Addition of 1 mM fresh FeMeOH (0.2 μmol) is enough to achieve the same performance level as with 1 week old cells (the amount of printed mediator is approximately 1.3 μmol per electrode) which shows that the enzyme is still active; 0.2 μmol of FeMeOH alone is not enough to produce the electrical energy (25 μA h) discharged during the CP measurement.

However, 1 and 2 weeks old 1 mM FeMeOH solutions did not increase the cell performance as much. This indicates that FeMeOH rapidly either loses its ability to work as an electron shuttle between the enzyme and the carbon particles or there is a chemical reaction that changes the FeMeOH to another compound which has a higher redox potential (300–350 mV vs. Ag/AgCl) than that of FeMeOH (200–250 mV vs. Ag/AgCl [42]).

Stability of ferrocene-based mediator has been studied earlier. Wang et al. [45] and Patel et al. [26] developed ferrocene-based systems showing 70% and 75% of the initial activity after one month as samples were stored at 4 °C and 25 °C, respectively. A study by Li et al. [22] reported a $Fe(CN)_3^{3-/4-}$-based sensor retaining 78% of its initial performance after one month (stored at 4 °C).

Table 2
Cells measured during this work.

	Anode	Age	Cathode	Age	Number of cells	Printing substrate (electrode size)	Measurement
Cell 1	Pilot ink 1	1 wk	Pilot ink	1 wk	3	Cardboard (9 cm^2)	CA
Cell 2	Pilot ink 1	1 wk	Pilot ink	1 wk	6	Cardboard (9 cm^2)	CP, 10 μA
Cell 3	Pilot ink 1	3 wk	Pilot ink	3 wk	3	Cardboard (9 cm^2)	CP, 10 μA
Cell 4	Pilot ink 1	5 wk	Pilot ink	5 wk	3	Cardboard (9 cm^2)	CP, 10 μA
Cell 5	Pilot ink 1	11 wk	Pilot ink	11 wk	3	Cardboard (9 cm^2)	CP, 10 μA
Cell 6	Pilot ink 1	13 wk	Pilot ink	13 wk	3	Cardboard (9 cm^2)	CP, 10 μA
Cell 7	Pilot ink 1	13 wk	Pilot ink	1 d	3	Cardboard/insulator paper (9 cm^2)	CP, 10 μA
Cell 8	Pilot ink 1	1 d	Pilot ink	13 wk	3	Insulator paper/cardboard (9 cm^2)	CP, 10 μA
Cell 9	Exp ink 10 wt% chit	1 d	Pilot ink	1 d	3	Insulator paper (12.25 cm^2)	CP, 15 μA
Cell 10	Exp ink 10.09 wt% chit	1 d	Pilot ink	1 d	3	Insulator paper (12.25 cm^2)	CP, 15 μA
Cell 11	Exp ink 10.17 wt% chit	1 d	Pilot ink	1 d	3	Insulator paper (12.25 cm^2)	CP, 15 μA
Cell 12	Exp ink 10.26 wt% chit	1 d	Pilot ink	1 d	3	Insulator paper (12.25 cm^2)	CP, 15 μA
Cell 13	Exp ink 10.34 wt% chit	1 d	Pilot ink	1 d	3	Insulator paper (12.25 cm^2)	CP, 15 μA
Cell 14	Exp ink 20.01 μmol nkatFeMeOH	1 d	Pilot ink	1 d	3	Insulator paper (12.25 cm^2)	CA
Cell 15	Exp ink 20.03 μmol nkatFeMeOH	1 d	Pilot ink	1 d	3	Insulator paper (12.25 cm^2)	CA
Cell 16	Exp ink 20.05 μmol nkatFeMeOH	1 d	Pilot ink	1 d	3	Insulator paper (12.25 cm^2)	CA
Cell 17	Exp ink 20.08 μmol nkatFeMeOH	1 d	Pilot ink	1 d	3	Insulator paper (12.25 cm^2)	CA
Cell 18	Exp ink 30 wt% chit	1 d	Pilot ink	1 d	3	Insulator paper (12.25 cm^2)	CP, 15 μA
Cell 19	Exp ink 30.13 wt% chit	1 d	Pilot ink	1 d	3	Insulator paper (12.25 cm^2)	CP, 15 μA
Cell 20	Exp ink 30.27 wt% chit	1 d	Pilot ink	1 d	3	Insulator paper (12.25 cm^2)	CP, 15 μA
Cell 21	Exp ink 30.40 wt% chit	1 d	Pilot ink	1 d	3	Insulator paper (12.25 cm^2)	CP, 15 μA
Cell 22	Exp ink 30.53 wt% chit	1 d	Pilot ink	1 d	3	Insulator paper (12.25 cm^2)	CP, 15 μA
Cell 23	Pilot ink 2	1 wk	Pilot ink	19 wk	3	Cardboard (9 cm^2)	CA
Cell 24	Pilot ink 2	1 wk	Pilot ink	19 wk	3	Cardboard (9 cm^2)	CP, 10 μA
Cell 25	Pilot ink 2	3 wk	Pilot ink	21 wk	3	Cardboard (9 cm^2)	CP, 10 μA
Cell 26	Pilot ink 2	5 wk	Pilot ink	23 wk	3	Cardboard (9 cm^2)	CP, 10 μA

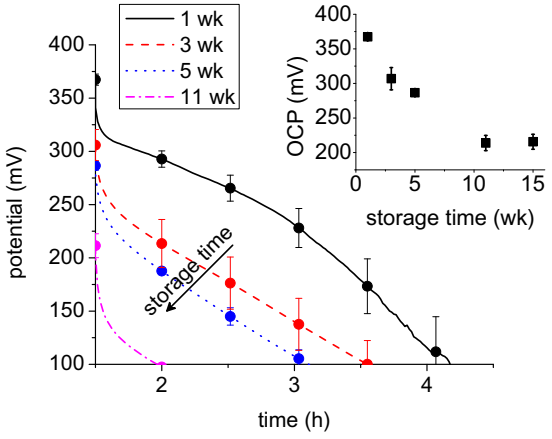

Fig. 3. Curves of chronopotentiometric measurement (constant current of 10 μA) and OCP (inset) of aged GOx/EcoL cells. Pilot anode ink 1 was used in these cells. The geometrical area of the cells was 9 cm^2. The data points represent mean ± SM (n = 3–6).

Chen et al. [4] demonstrated a FeMeOH-based creatinine biosensor which showed 94% of the initial current after more than 6 month storage period as dry at room temperature. These studies indicate that the ferrocene-based redox-systems are fairly stable.

On the other hand, lyophilized GOx is very stable; at 0 °C it is stable for 2 years and at −15 °C for 8 years [2]. In solution the stability of GOx is dependent on the pH; it is most stable at around pH 5 [49]. In a study by Liu et al. [23] there was nearly no decrease in the GOx-based biosensor after storing the biosensor for 15 days at 4 °C. Lawrence et al. [21] reported 98% of the initial performance of a GOx-based biosensor after four months (stored at 4 °C as dry). In a study presented by Onda et al. [25], GOx was assembled with polycations in the preparation of molecular films. The films that were stored in water at 25 °C showed drastic decrease in activity, and approximately only 30% of the activity was retained after 4 weeks. The films which were kept in a buffer at 4 °C did not show a significant decrease in enzymatic activity over 14 weeks. The films stored in air at 4 °C showed 10% decrease in the first week

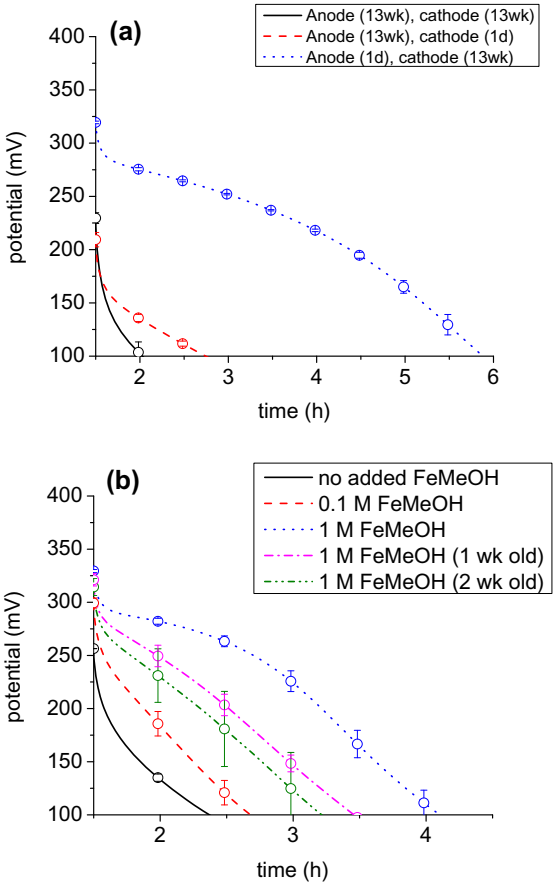

Fig. 4. Curves of chronopotentiometric measurement (constant current of 10 μA) of GOx/EcoL cells (a) as aged (13 weeks old) and fresh electrodes (1 day old) were tested together and (b) as aged (15 weeks old) electrodes were tested with fresh and aged FeMeOH in the activation electrolyte. Geometrical area of the cells was 9 cm^2. The data points represent mean ± SM (n = 3).

but the activity was maintained during the following 13 weeks. The conclusion is that the stability of GOx-based bioelectronics is highly dependent on the storing conditions, and low storing temperature seems to be the key factor.

R2R screen-printed GOx-electrodes without FeMeOH (dried at around 70 °C during the printing process) retained approximately 60% of their initial activity as stored dry for one month (both at room temperature and 4 °C) [42]. However, the presence of FeMeOH in the GOx-electrodes reduced the performance to approximately 30% after one month. This leads to a conclusion that the FeMeOH is the limiting factor in the case of storing stability of GOx-electrodes. The reason for this is still unknown and this phenomenon will be studied in the future. We speculate that FeMeOH gets protonated during the ink preparation process by the succinic acid (dicarboxylic acid) used for the stabilisation of GOx. This reaction leads to elimination the hydroxyl group from FeMeOH forming α-ferrocenyl carbocation (S_N1 reaction on FeMeOH has been studied by Peljo et al. [28]). The formed α-ferrocenyl carbocation reacts with the dicarboxylic acid forming an insoluble ferrocenecarboxylic acid compound, and thus leads to increase in the redox potential of the mediator. Ferrocenecarboxylic acid has a redox potential close to 350 mV vs. Ag/AgCl and has a voltammetric response with GOx starting at 300 mV vs. Ag/AgCl [42]. This potential correlates well with the OCP of the aged cells.

Moreover, a reaction between α-ferrocenyl carbocation and the cofactor of GOx (FAD) is also possible leading to denaturation of GOx. If the enzyme and/or the mediator could be stabilised the anode electrodes were more stable. For this reason, addition of chitosan into experimental anode inks was tested in order to increase stability. This topic is discussed more in the next chapter.

3.2. Optimisation of the anode ink

Experimental inks for the anode were made in order to improve the printability and mechanical stability of the printed anode layer, as well as enzyme and mediator stability. Adhesive behaviour of graphite-based inks can be tailored by controlling the binder to graphite ratio [30]. In addition, ink composition affects also stability as delamination of thin films increases in moist environment [46]. Adding hydrophobic chitosan into the experimental anode inks was tested to improve adhesive behaviour of the electrode. This is kind of a passive corrosion protection which is typically done by fabricating a hydrophobic film that prevents wetting and direct contact with water and/or corrosive liquids thus decreasing corrosion (Samyn [37]). For an example, Höhne et al. [12] synthesized superhydrophobic aluminium surfaces by depositing a chitosan layer and poly(octadecene-alt-maleic anhydride) on microroughened substrates. Ivanova and Philipchenko [15] developed a method to make hydrophobic fabrics by using chitosan-based hydrophobic nanoparticles. Song et al. [40] used chitosan-based polymer to prepare durable superhydrophobic films using a simple and low-cost phase separation method. Hence, chitosan has been used in many applications in order to add hydrophobicity to surfaces.

Chitosan has also been successfully used as an immobilisation and stabilisation polymer-matrix for enzymes [11,22,23,34,35,38,43,47] as well as for iron-based redox couples [11,22,45] in numerous studies. In the perspective of enzymes, PEO is essentially an inert hydrophilic polymer [14], whereas chitosan is hydrophobic, pseudo-natural cationic polymer [8,33]. In hydrophobic solvents a higher amount of water remains associated with the enzyme structure, and thus they exhibit higher activity in hydrophobic solvents than in hydrophilic ones [32]. Additionally, cationic chitosan is a suitable polymer for anionic GOx (pKa 4.2 [27]) because of attractive forces induced by their opposite charges. Hence, hydrophobic characteristic of a chitosan-containing ink can protect the enzyme from dehydration and prevent denaturation.

Moreover, chitosan may act as a stabiliser for FeMeOH. Chitosan has nucleophilic amino groups that can be modified by mild chemical reactions [31]. A chemical synthesis of a ferrocene-chitosan based derivative is also possible [52] as well as a mild synthesis process of a lactic acid-grafted chitosan copolymer [3]. Bhattarai et al. [3] dehydrated chitosan lactate salts for copolymerisation using heat (70–90 °C) to form an amide linkage. This synthesis process is very close to our electrode preparation process where chitosan is mixed with succinic acid (at pH 4.5) and FeMeOH. During the ink drying process one carboxylic acid functional group of succinic acid molecule can react with one amine group of chitosan and the other with α-ferrocenyl carbocation

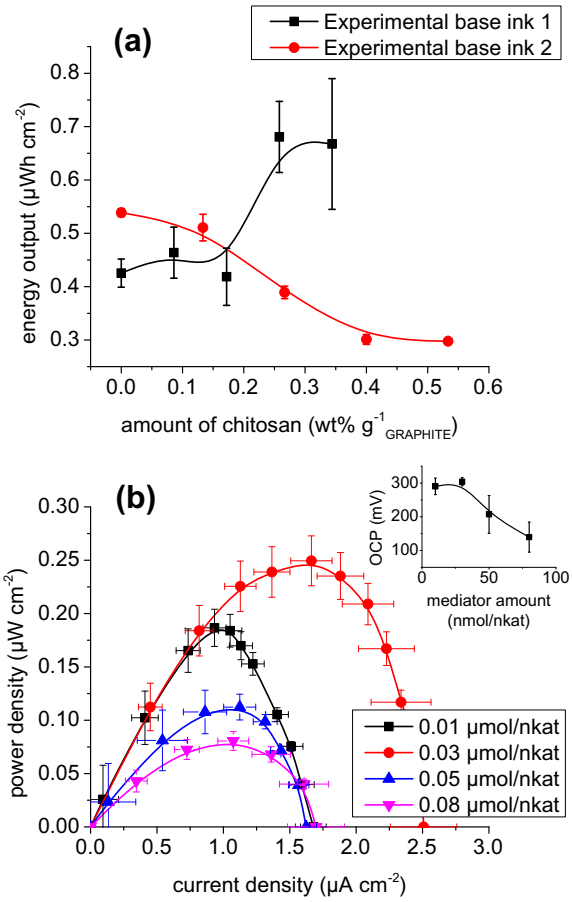

Fig. 5. (a) Energy outputs calculated from chronopotentiometric measurement (constant current of 15 μA, $E_{cut\text{-}off}$ = 150 mV) of experimental base inks containing different amounts of PEO and chitosan. (b) Curves of chronoamperometric measurement and OCP (inset) of experimental inks containing different amounts of FeMeOH. Geometrical area of the cells was 12.25 cm^2. The data points represent mean ± SM (n = 3).

Table 3
Average thickness and roughness of pilot printed anode ink 2 layers. The errors are calculated standard deviations. The values of the pilot anode ink 1 are reprinted from Tuurala et al. [42] with permission.

	Anode ink 1	Anode ink 2
Thickness (μm)	103 ± 22	98 ± 21
Ra[a]	9 ± 1	5.8 ± 0.7
Rq[b]	11 ± 3	7 ± 1

[a] Aritmetic mean.
[b] Quatratic mean.

forming a stabilised ferrocene-chitosan derivative. It must be emphasised though that this reaction has not been verified and will be studied in more detail in the future.

Addition of different amounts of chitosan and FeMeOH into the anode ink was tested in order to increase printability, adhesion and stability of the anode layers. CP and CA curves of three different experimental anode inks are presented in Fig. 5. It can be seen that addition of chitosan into the PEO-containing inks has effect on the energy output (Fig. 5a). If there is low amount of PEO (3.6 wt% $g^{-1}_{GRAPHITE}$) in the ink, increasing amount of chitosan increases the energy output. On the other hand, if there is a high amount of PEO (7 wt% $g^{-1}_{GRAPHITE}$) in the ink, increasing the amount of chitosan decreases the energy output. However, in all the cases higher amount of chitosan in the ink makes the printing process better and increases the ink adhesion to the printing substrate. For this reason, addition of small amount of chitosan is needed for good printing process and print quality.

Addition of different amounts of FeMeOH into the ink was also tested and it can be seen that there is a clear optimum (Fig. 5b). For this particular ink composition, 0.03 μmol $nkat^{-1}$ (of GOx enzyme activity) is the optimum. If the mediator amount is increased further there is significant drop in the power density most probably due to denaturation of the enzyme by the excess amount of the mediator. For this reason, 0.02 μmol $nkat^{-1}$ (of GOx enzyme activity) was seen as a safe amount of FeMeOH for the pilot anode ink 2.

3.3. Performance of the pilot anode ink 2

On the bases of the anode ink optimisation experiments, the amount of binder was doubled and in addition to PEO small amount of chitosan was used in the pilot anode ink 2. Furthermore, the amount of anodic mediator per dry ink was approximately 2-fold compared to the pilot anode ink 1 to increase the cell performance and stability. From the point of view of the printing process, PEO seems to function well as a flow-adding component whereas chitosan adds viscosity to the ink. Thus combination of PEO and chitosan resulted in better ink-flow and printing quality compared to the pilot anode ink 1.

The thickness of the new anode layer was the same as in the previous batch (see Table 3). However, the roughness of the new anodes was 36% lower than that of the anodes using pilot anode ink 1. In addition, the surface topography (see Fig. 6) shows that the difference between the highest and the lowest point of the surface is around 50 μm whereas it was roughly 80 μm in the anodes printed using the pilot ink 1 [42]. This means that the pilot anode

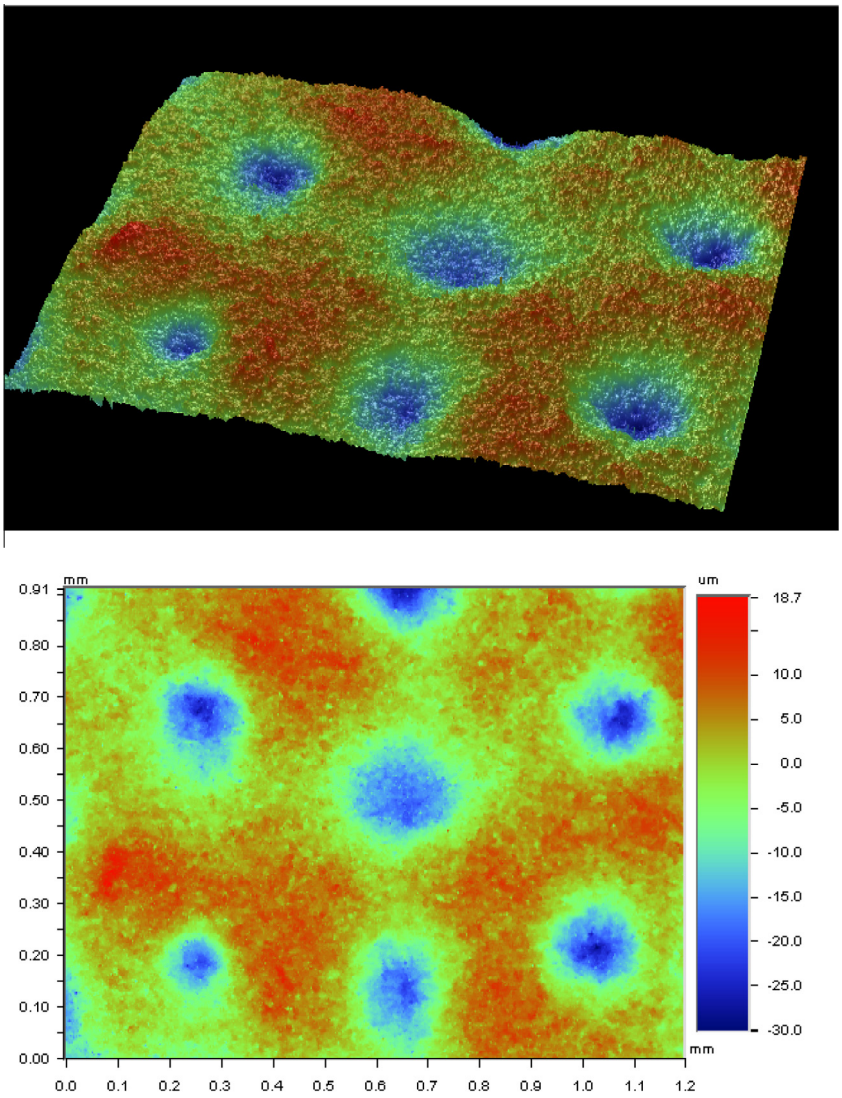

Fig. 6. An optical image (magnification 5.2) of the surface (0.91 mm × 1.20 mm) of the anode layer printed using the pilot anode ink 2 on cardboard. The equivalent image of the anode layer printed using the pilot anode ink 1 can be seen in the Supplementary material 5 (Fig. 3) of our previous publication [42].

ink 2 settles better than the pilot anode ink 1 during printing process leading to more even print quality.

The electrochemical performance of the new anode batch was also studied. The OCP of the 1 week old pilot cells is (341 ± 1) mV and the maximum power density is (0.59 ± 0.02) μW cm^{-2} (at 200 mV). The OCP is the same whereas the maximum power density is 1.5-fold compared to the cells fabricated using the pilot anode ink 1 (see Fig. 7a). The energy outputs calculated from CP measurements (Fig. 7b) are (0.88 ± 0.01) μW h cm^{-2} ($E_{cut\text{-}off}$ = 200 mV) and (1.07 ± 0.02) μW h cm^{-2} ($E_{cut\text{-}off}$ = 150 mV), which are 1.5-fold and 1.6-fold compared to those obtained with the pilot anode ink 1, respectively. The increase in the electrochemical performance is most probably due to 1.75-fold amount of mediator per electrode compared to the mediator amount per electrode in the case of the pilot anode ink 1. In addition, these values are in good correlation with the laboratory manufactured cells (see Section 3.2). Both the maximum power density and the energy output ($E_{cut\text{-}off}$ = 150 mV) are approximately two times higher than that of laboratory manufactured cells which is explained by the different printing screens. The ink layer is two times thicker in the case of pilot printing; hence there is two times more enzyme and mediator in the pilot printed electrodes.

Although we were able to increase the performance of the printed bioanodes, the values achieved seem modest compared to power densities of glucose/O_2 biofuel cells studied by other research groups. For an example, Zhou et al. [55] has demonstrated

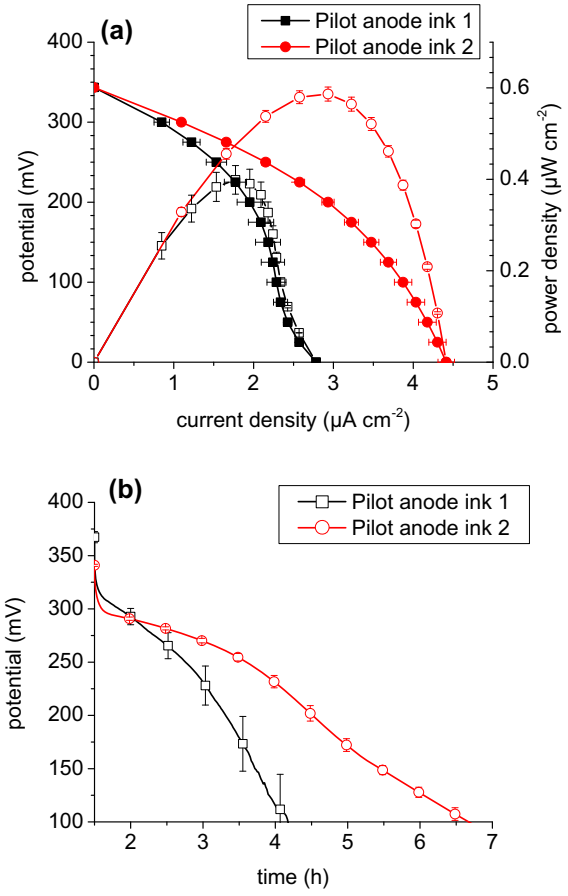

Fig. 7. (a) Potential curve (*full symbols*) and power curve (*hallow symbols*) of chronoamperometric measurement, and (b) chronopotentiometric (constant current of 10 μA) measurement of pilot printed GOx/EcoL cells. Two different pilot anode inks were used. Part of the results of the pilot anode ink 1 were previously published by Tuurala et al. [42] and they are presented here with permission. Geometrical area of the cells was 9 cm^2. The data points represent mean ± SM (n = 3–6).

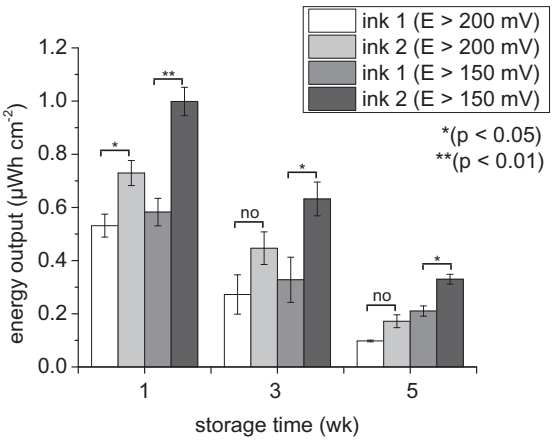

Fig. 8. Energy output calculated from chronopotentiometric measurement (constant current of 10 μA) of pilot printed GOx/EcoL cells versus storage time. Two different pilot anode inks were used. The data points represent mean ± SM (n = 3–6). The p represents the p-value of Student's t-test.

a glucose dehydrogenase (GDH) laccase cell based on highly ordered mesoporous carbon with power density of 38.7 μW cm^{-2}. Sakai et al. [36] build a high-power GDH/laccase cell based on carbon-fibre sheets which resulted in power density of 1.45 mW cm^{-2}. In addition, Zebda et al. [54] fabricated a high-power mediatorless GOx/laccase cell based on compressed multi-walled carbon nanotubes and demonstrated a power density of 1.3 mW cm^{-2}. We want to emphasise though that they used much higher amount of enzyme on the anodes than us; as the power output is calculated by anode enzyme activity the numbers are different 2.3 μW U^{-1}, 12.9 μW U^{-1} and 0.3 μW U^{-1}, respectively. Our bioelectrodes contain approximately 0.7 U cm^{-2} of enzyme activity and thus the power output is 0.8 μW U^{-1}. In addition, the anode is 20–30 times thicker than in our case, which means smaller amount of electrolyte in the anode compartment and thus higher mass-transfer limitations.

We have previously reported an OCP, maximum power density and energy output of (380 ± 8) mV, (1.4 ± 0.1) μW cm^{-2} and (5.5 ± 0.2) μW h cm^{-2}, respectively, for laboratory manufactured cells [42]. The amount of GOx and FeMeOH in the electrodes produced in laboratory was approximately 0.6- and 4-fold, respectively, compared to the pilot anode ink 2. In addition, the laboratory-manufactured cells were printed on a different substrate and dried at room temperature. Because there are many variables that have been changed (the amount of enzyme and mediator, printing substrate and drying temperature), interpretation of the differences in the electrochemical performance is not straightforward. However, these previous results together with the above described experiments with the different FeMeOH concentrations (Figs. 4 and 5b) show that the amount of the mediator plays an important role in the performance and stability of the GOx-electrodes.

In addition to improved electrochemical behaviour, higher binder amount results in a more rigid anode ink layer, decreasing the delamination of the enzymatic layer from the conductive current collector layer. This is observed as more reproducible samples (i.e. decreased error bars in Fig. 7) and significantly higher energy outputs for stored samples as shown in Fig. 8. However, due to the degradation process of the anode mediator the cells degrade at the same pace regardless of the anode ink used.

3.4. Conclusions

R2R printed enzymatic electrodes were manufactured on a cardboard material. During assembling the cells it was observed

that the anode ink layer cracked very easily as dry rendering the assembling of the cells difficult. The anode ink was also very water soluble which decreases the functionality and operational lifetime of the cells, because the enzyme was not immobilized properly into the ink and the conductive layer was lost. The cathode ink layer was more rigid than the anode ink and did not show any problems during the cell assembly. In addition, the electrochemical performance of the cells decreased dramatically during the storage due to the self-degradation of the anodic mediator.

Due to the challenges with the first pilot anode ink a new pilot anode ink was fabricated containing two times more binder than the initial one. In addition to PEO a small amount of chitosan was added to the ink to increase the viscosity (i.e. better printability) and adhesion of the ink as well as the enzyme and mediator stability. Furthermore, two times higher amount of the mediator was used compared to the initial anode ink, which lead to 1.75 times higher amount of the mediator per each electrode. The new anode ink was tested in the R2R printing process and it functioned better than the initial anode ink; the printed layers became more rigid and did not crack during the assembly. In addition to more facile printing process, approximately 1.5 times higher electrochemical performance was obtained with the cells fabricated from the latter ink compared to ones using the initial anode ink. Moreover, the stability and reproducibility of the cells was increased. However, the stability of the anode mediator was not increased.

In the future, degradation of the anode side mediator will be studied in more detail in order to increase the stability of the cells. On the other hand, adding fresh mediator into the biobatteries during their activation was shown to improve the performance, but from the user point of view it is not practical. Another possibility could be adding the mediator as a separate dry layer, as it is storable as dry.

Conflict of interest

None declared.

Acknowledgements

Tiina Maaninen, Pekka Ontero, Mikko Hietala and Arto Ranta-Panula (VTT) are thanked for their assistance in the R2R manufacturing and characterisation of enzymatic electrodes. In addition, Asta Pesonen (VTT), Anu Vaari (VTT) and Prof. Kyösti Kontturi (Aalto University) are gratefully thanked for technical and academic assistance. The research was funded by the Printed Enzymatic Power Source with embedded capacitor on next generation devices – Project (PEPSecond) supported by Tekes, the Finnish Funding Agency for Technology and Innovation.

References

[1] R.L. Arechederra, S.D. Minteer, Anal. Bioanal. Chem. 400 (2011) 1605–1611.
[2] R. Bentley, Glucose oxidase, in: P. Boyer, H. Lardy, K. Myrback (Eds.), The Enzymes, Academic Press, New York, 1963, p. 567.
[3] N. Bhattarai, H.R. Ramay, S.-H. Chou, M. Zhang, Int. J. Nanomed. 1 (2006) 181–187.
[4] P. Chen, Y. Peng, M. He, X. Yan, Y. Zhang, Y. Liu, Int. J. Electrochem. Sci. 8 (2013) 8931–8939.
[5] M.J. Cooney, V. Svoboda, C. Lau, G. Martin, S.D. Minteer, Energy Environ. Sci. 1 (2008) 320.
[6] W. Dungchai, O. Chailapakul, C.S. Henry, Anal. Chem. 81 (2009) 5821–5826.
[7] W. Dungchai, O. Chailapakul, C.S. Henry, Anal. Chim. Acta 674 (2010) 227–233.
[8] P. Dutta, J. Dutta, V. Tripathi, J. Sci. Ind. Res. (India) 63 (2004) 20–31.
[9] L. Feng, X. Li, H. Li, W. Yang, L. Chen, Y. Guan, Anal. Chim. Acta 780 (2013) 74–80.
[10] D. Grieshaber, R. MacKenzie, J. Voeroes, E. Reimhult, Sensors 8 (2008) 1400–1458.
[11] M. Hedström, F. Plieva, I.Y. Galaev, B. Mattiasson, Anal. Bioanal. Chem. 390 (2008) 907–912.
[12] S. Höhne, C. Blank, A. Mensch, M. Thieme, R. Frenzel, H. Worch, M. Müller, F. Simon, Macromol. Chem. Phys. 210 (2009) 1263–1271.
[13] A. Illanes, Electron. J. Biotechnol. 2 (1999) 7–15.
[14] J. Israelachvili, Proc. Natl. Acad. Sci. 94 (1997) 8378–8379.
[15] N.A. Ivanova, A.B. Philipchenko, Appl. Surf. Sci. 263 (2012) 783–787.
[16] P. Jenkins, S. Tuurala, A. Vaari, M. Valkiainen, M. Smolander, D. Leech, Enzyme Microb. Technol. 50 (2012) 181–187.
[17] P. Jenkins, S. Tuurala, A. Vaari, M. Valkiainen, M. Smolander, D. Leech, Bioelectrochemistry 87 (2012) 172–177.
[18] E. Katz, A. Bückmann, I. Willner, J. Am. Chem. Soc. 123 (2001) 10752–10753.
[19] M.S. Khan, S.B.M. Haniffa, A. Slater, G. Garnier, Colloids Surf. B 79 (2010) 88–96.
[20] M.S. Khan, X. Li, W. Shen, G. Garnier, Colloids Surf. B 75 (2010) 239–246.
[21] C.S.K. Lawrence, S.N. Tan, C.Z. Floresca, Sens. Actuators B 193 (2014) 536–541.
[22] W. Li, R. Yuan, Y. Chai, L. Zhou, S. Chen, N. Li, J. Biochem. Biophys. Methods 70 (2008) 830–837.
[23] Y. Liu, M. Wang, F. Zhao, Z. Xu, S. Dong, Biosens. Bioelectron. 21 (2005) 984–988.
[24] A.W. Martinez, S.T. Phillips, G.M. Whitesides, E. Carrilho, Anal. Chem. 82 (2010) 3–10.
[25] M. Onda, K. Ariga, T. Kunitake, J. Biosci. Bioeng. 87 (1999) 69–75.
[26] H. Patel, X. Li, H.I. Karan, Biosens. Bioelectron. 18 (2003) 1073–1076.
[27] J.H. Pazur, K. Kleppe, Biochemistry 3 (1964) 578–583.
[28] P. Peljo, L. Qiao, L. Murtomäki, C. Johans, H.H. Girault, K. Kontturi, Chemphyschem 14 (2013) 311–314.
[29] K.M. Polizzi, A.S. Bommarius, J.M. Broering, J.F. Chaparro-Riggers, Curr. Opin. Chem. Biol. 11 (2007) 220–225.
[30] J. Rangel, A. Del-Real, V. Castano, Chem. Chem. Technol. 2 (2008) 305–308.
[31] M. Rekha, C. Sharma, Trends Biomater. Artif. Organs 21 (2008) 107–115.
[32] K. Rezaei, E. Jenab, F. Temelli, Crit. Rev. Biotechnol. 27 (2007) 183–195.
[33] M. Rinaudo, Prog. Polym. Sci. 31 (2006) 603–632.
[34] R.A. Rincón, C. Lau, H.R. Luckarift, K.E. Garcia, E. Adkins, G.R. Johnson, P. Atanassov, Biosens. Bioelectron. 27 (2011) 132–136.
[35] R.A. Rincón, C. Lau, K.E. Garcia, P. Atanassov, Electrochim. Acta 56 (2011) 2503–2509.
[36] H. Sakai, T. Nakagawa, Y. Tokita, T. Hatazawa, T. Ikeda, S. Tsujimura, K. Kano, Energy Environ. Sci. 2 (2009) 133–138.
[37] P. Samyn, J. Braz. Chem. Soc. 25 (5) (2014) 947–960.
[38] K. Sjoholm, M. Cooney, S. Minteer, ECS Trans. 19 (2009) 1–7.
[39] M. Smolander, H. Boer, M. Valkiainen, R. Roozeman, M. Bergelin, J.-E. Eriksson, X.-C. Zhang, A. Koivula, L. Viikari, Enzyme Microb. Technol. 43 (2008) 93–102.
[40] W. Song, V.S. Gaware, Ö.V. Rúnarsson, M. Másson, J.F. Mano, Carbohyd. Polym. 81 (2010) 140–144.
[41] A. Swerin, I. Mira, Sens. Actuators B 195 (2014) 389–395.
[42] S. Tuurala, O.-V. Kaukoniemi, L. von Hertzen, J. Uotila, A. Vaari, M. Bergelin, P. Sjöberg, J.-E. Eriksson, M. Smolander, J. Appl. Electrochem. 44 (2014) 881–892.
[43] S. Tuurala, C. Lau, P. Atanassov, M. Smolander, S.D. Minteer, Electroanalysis 24 (2012) 229–238.
[44] S. Tuurala, M. Smolander, J. Uotila, O.-V. Kaukoniemi, H. Boer, M. Valkiainen, A. Vaari, A. Koivula, P. Jenkins, ECS Trans. 25 (2010) 1–10.
[45] H. Wang, Q. Pan, G. Wang, Sensors 5 (2005) 266–276.
[46] P. Waters, The Effects of Moisture on Thin Film Delamination and Adhesion, University of South Florida, 2005.
[47] R. Vazquez-Duhalt, R. Tinoco, P. D'Antonio, L.D. Topoleski, G.F. Payne, Bioconjugate Chem. 12 (2001) 301–306.
[48] I. Willner, E. Katz (Eds.), Bioelectronics: From Theory to Applications, WILEY-VCH, Weinheim, 2005.
[49] R. Wilson, A. Turner, Biosens. Bioelectron. 7 (1992) 165–185.
[50] H. Virtanen, H. Orelma, T. Erho, M. Smolander, Process Biochem. 47 (2012) 1496–1502.
[51] H. Virtanen, K. Vehmas, T. Erho, M. Smolander, Packag. Technol. Sci. 27 (2014) 819–830.
[52] W. Yang, H. Zhou, C. Sun, Macromol. Rapid Commun. 28 (2007) 265–270.
[53] A.K. Yetisen, M.S. Akram, C.R. Lowe, Lab Chip 13 (2013) 2210–2251.
[54] A. Zebda, C. Gondran, A. Le Goff, M. Holzinger, P. Cinquin, S. Cosnier, Nat. Commun. 2 (2011) 370.
[55] M. Zhou, L. Deng, D. Wen, L. Shang, L. Jin, S. Dong, Biosens. Bioelectron. 24 (2009) 2904–2908.
[56] M. Zhou, S. Dong, Acc. Chem. Res. 44 (2011) 1232–1243.
[57] M. Zhou, J. Wang, Electroanalysis 24 (2012) 197–209.